

- [24] $\text{LiF}:\text{OH}^-$,^[6] CaF_2 ,^[7, 13, 17] $\text{CaSO}_4 \cdot 0.5\text{H}_2\text{O}$,^[8, 11] BaF_2 ,^[9, 10] BaSO_4 ,^[11] SiO_2 surface,^[12] $\text{Si}_8\text{O}_{12}\text{R}_8$ -cage,^[14, 18] SiO_2 high-pressure modifications,^[15, 16] $\text{NaAl}_3(\text{OH})_4(\text{PO}_4)_2$,^[19] Li_2O ,^[20, 21] $\text{LiF}:\text{H}^-$, Mg^{2+} .^[22, 23]
- [25] H. Dilger, E. Roduner, R. Scheuermann, J. Major, M. Schefzik, R. Stöber, M. Päch, D. G. Fleming, *Phys. Condens. Matter* **1999**, in press.
- [26] R. Stöber, J. Bartoll, L. Schirmermeister, R. Ernst, R. Lück, *Appl. Radiat. Isot.* **1996**, *47*, 1489–1496.
- [27] P. J. Bruna, G. H. Lushington, F. Grein, *Chem. Phys. Lett.* **1996**, *258*, 427–430.
- [28] Detectable as satellites on the hyperfine lines of the H^\cdot atoms.^[18]
- [29] F. J. Adrian, *J. Chem. Phys.* **1960**, *32*, 972–981.

Intermediate-Range Order in Amorphous Nitridic Ceramics: Lessons from Modern Solid-State NMR Spectroscopy**

Leo van Wüllen, Utz Müller, and Martin Jansen*

Structural characterization and theoretical modeling of crystalline solids are only possible because of their translational symmetry. Once the translational periodicity is lost, as in quasicrystals and amorphous networks, the structural characterization of these solids, a prerequisite for a profound understanding of the physical and chemical properties, becomes a rather tedious task. This lack of routine methods for the structural characterization of amorphous solids is the reason for an only limited understanding of scientifically and industrially important systems.

Amorphous ceramics in the system boron, silicon, carbon, and nitrogen have gained considerable importance as high-performance ceramic materials due to their exceptional stability at high temperatures and their resistance to oxidation.^[1] Among these ceramics, those obtained by ammonolysis, polycondensation, and subsequent pyrolysis of single-source precursors have been ascribed superior characteristics with respect to resistance to crystallization and homogeneity.^[2] The ternary ceramic $\text{Si}_3\text{B}_3\text{N}_7$ and the quaternary ceramic SiBN_3C are the best studied so far with respect to structural details.^[3] A structural characterization of these amorphous systems can only be successful if a combination of characterization methods is used, each predominantly probing the short-, intermediate-, or long-range order. Modern solid-state NMR spectroscopy is emerging as one of the most powerful tools in this field. The short-range order in a range of 1–2 Å was successfully elucidated by magic angle spinning (MAS)

NMR methods. These studies found trigonally planar BN_3 and tetrahedral SiN_4 polyhedra as the basic building blocks constituting the network. Transmission electron spectroscopy studies revealed^[4] that the amorphous network in these ceramics is homogeneous with respect to an elemental distribution on a subnanometer scale. To date, the intermediate-range order, corresponding to a length scale of 2–5 Å has not yet been accessible. This gap is closed with the present study, by utilizing modern double resonance solid-state NMR methods. As a first characterization of the ceramic $\text{Si}_3\text{B}_3\text{N}_7$ the solid-state NMR single-pulse MAS solid-state spectra were recorded. The signals with isotropic chemical shifts of $\delta = -45.2$ (^{29}Si MAS-NMR) and 30.4 (^{11}B MAS NMR) indicate a local environment consisting of BN_3 and SiN_4 units, as confirmed by a comparison to the spectra of the binary model compounds h-BN and $\alpha\text{-Si}_3\text{N}_4$ and $\beta\text{-Si}_3\text{N}_4$, respectively.^[5]

The intermediate-range order, originating in the interconnection of the polyhedra to give the resulting amorphous network, was traced by employing rotational echo double resonance (REDOR) NMR spectroscopy.^[6] In this approach, the heteronuclear dipolar interaction between two nuclear species I and S, averaged out under the conditions of the MAS experiment, is reintroduced by rotor-synchronized 180° dephasing pulses for the S spins. The signal of the first nuclear species I is detected by using a rotor-synchronized solid-state spin-echo pulse sequence. The 180° pulses for the second nuclear species (S) produce a sign shift of the heteronuclear dipolar Hamiltonian, resulting in a decreased echo amplitude S . A conventional spin echo experiment for the I spins provides the maximum echo amplitude S_0 . Simulations of the resulting dipolar evolution curve, obtained as a plot of the normalized difference $\Delta S/S_0$ as a function of the dipolar evolution time—the product of the number of rotor cycles N and the rotor period T_R —then allows a direct determination of the ^{11}B - ^{29}Si internuclear distance in the case of an isolated two-spin system. Comparing the two principally feasible experiments $^{29}\text{Si}\{^{11}\text{B}\}$ -REDOR and $^{11}\text{B}\{^{29}\text{Si}\}$ -REDOR NMR the first would be the natural choice because of the natural abundance of the two isotopes ^{29}Si (4.7%) and ^{11}B (80.4%). The quadrupolar nature of the isotope ^{11}B (nuclear spin = 3/2) as the dephasing nucleus however severely complicates data analysis.^[7] Therefore we decided to perform the second variant, $^{11}\text{B}\{^{29}\text{Si}\}$ REDOR. This makes the use of a 100% ^{29}Si isotopically enriched sample of $\text{Si}_3\text{B}_3\text{N}_7$ vital, since in a $^{11}\text{B}\{^{29}\text{Si}\}$ -REDOR experiment on a sample containing ^{29}Si in natural abundance only approximately 5% of the actual B-Si dipolar couplings would be detected.

Figure 1 contains a compilation of $^{11}\text{B}\{^{29}\text{Si}\}$ -REDOR spectra for dipolar evolution times of 0.4, 1.2, and 2 ms together with the resulting REDOR curve. The lineshape of the ^{11}B resonance is dominated by the second-order quadrupolar interaction, which is not completely averaged out even under the conditions of fast MAS. Line shape analysis yields a quadrupolar coupling constant of 2.9 MHz and an asymmetry parameter η of 0.1. Figure 1a shows the results of ^{11}B -spin-echo experiments, Figure 1b the $^{11}\text{B}\{^{29}\text{Si}\}$ -REDOR spectra. The difference of the two experiments is plotted in Figure 1c. An increase of the difference intensity $S - S_0$ with increasing dipolar evolution time becomes obvious.

[*] Prof. Dr. M. Jansen, Dr. L. van Wüllen
Max-Planck-Institut für Festkörperforschung
Heisenbergstrasse 1, 70569 Stuttgart (Germany)
Fax: (+49) 711-689-1502
E-mail: martin@jansen.mpi-stuttgart.mpg.de
Dipl.-Chem. U. Müller
Institut für Anorganische Chemie
Rheinische Friedrichs-Wilhelms-Universität Bonn
Gerhard-Domagk-Strasse 1, 53121 Bonn (Germany)

[**] This work was supported by the Deutsche Forschungsgemeinschaft (SFB 408).

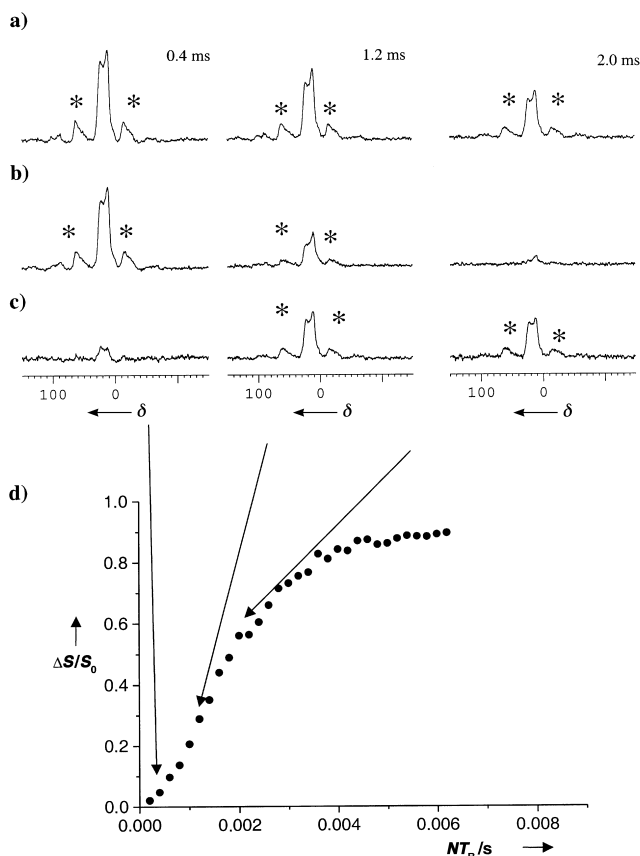


Figure 1. a) ^{11}B -spin-echo MAS spectra, b) $^{11}\text{B}\{^{29}\text{Si}\}$ REDOR NMR spectra with the 180° pulses applied on the ^{29}Si channel, c) difference spectra at evolution times of 0.4, 1.2, and 2 ms. d) Resulting REDOR curve.

An analysis of the REDOR curve only succeeds when multiple spin interactions are incorporated into the simulations. Trigonally planar boron, coordinated by nitrogen, can be coordinated to up to six silicon atoms in the second coordination sphere, so that multiple spin interactions up to a seven-spin system (BSi_6 interaction) principally have to be taken into account. Moreover, distribution of bond lengths and angles in amorphous networks further complicate interpretation of the data. Both effects result in a smearing out of the oscillations of the REDOR curves characteristic for isolated two-spin systems at long evolution times. Detailed calculations, however,^[8] reveal that the initial part of the REDOR curves is to a good approximation unaffected by distribution effects and exact angles in a given geometry of the multiple spin interactions. Consequently we restricted data analysis to $\Delta S/S_0$ values of up to about 0.5.

Figure 2 shows a comparison of the experimental data with simulations, obtained by assuming a B–Si two-spin system (dotted line) and a B– Si_2 three-spin interaction (dashed line), as well as a mean B–Si distance of 2.74 Å, a value, which is suggested by neutron diffraction data.^[9] The solid line corresponds to a weighted superposition of the above-mentioned models. The simulations lead to the surprising result that the boron atoms are connected (through the three nitrogen atoms) to an average number of 1.35 ± 0.2 silicon atoms. Thus, on an intermediate length scale, the amorphous network cannot be described by a homogenous elemental

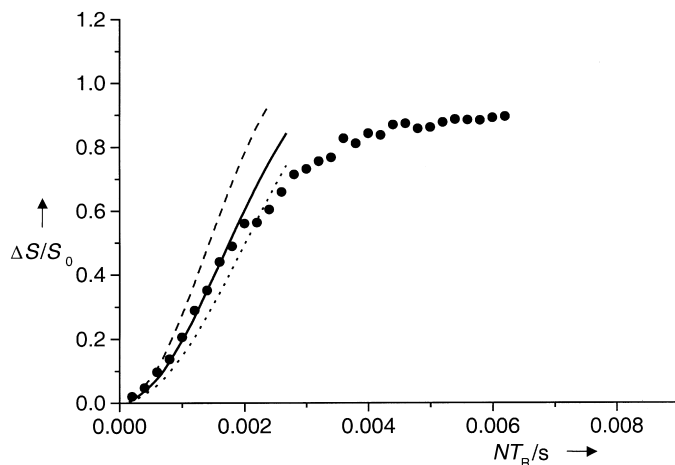


Figure 2. Experimental REDOR data (filled circles) together with simulations in which an isolated two-spin interaction (dotted curve) and a B– Si_2 three-spin interaction (dashed curve) are assumed. The solid line corresponds to a weighted superposition of the two simulations according to $\Delta S/S_0 = 0.38 \Delta S/S_0(\text{BSi}_2) + 0.62 \Delta S/S_0(\text{BSi})$. A B–Si internuclear distance of 2.74 Å was used in the calculations.

distribution. This would imply an average number of three silicon neighbors in the second coordination sphere of a central boron atom. However, the results are rather consistent with a formation of silicon-rich and boron-rich islands. This connectivity motif can be explained with the help of the kinetics of the ammonolysis of the BCl_2 and SiCl_3 groups in the precursor molecule trichlorosilylamino-dichloroborane (TADB). The higher Lewis acidity of the BCl_2 fragment implies a faster attack of ammonia at the boron site of TADB. As a consequence only B– NH_2 groups are available for the polycondensation at the beginning of the reaction, resulting in an oligomer, which is predominantly characterized by B–N–B linkages. Si–Cl bonds are not attacked by ammonia unless the local B–Cl supply is almost depleted. Thus, a network emerges, predominantly characterized by regions of B–N–B and regions of Si–N–Si linkages.

The results are supported by additional NMR experiments. Static ^{11}B spin-echo and ^{29}Si spin-echo experiments principally allow a determination of the number of homonuclear neighbors in the second coordination sphere and can therefore be used to support the double resonance data. Analysis of the ^{11}B spin-echo experiment results in an average number of 4.5 ± 0.5 boron atoms in the second coordination sphere of a central boron atom, whereas the analogous ^{29}Si spin-echo experiment indicates 6.5 ± 0.5 silicon atoms in the second coordination sphere of a central silicon atom. The single B–N–Si linkage already present in the single-source precursor molecule TADB seems to prevail during condensation and pyrolysis, while the new formed connectivities during the condensation process consist predominantly of B–N–B and Si–N–Si linkages. We emphasize the fact that the formation of the described islands is consistent with the previously found SiN_4 and BN_3 polyhedra as the short-range ordering motif and the homogenous elemental distribution down to a length scale of approximately 10 Å.

The presented results may have—apart from the structural characterization of a specific amorphous network, $\text{Si}_3\text{B}_3\text{N}_7$ —a

somewhat universal character, especially in terms of attempts to model amorphous structures exclusively on the basis of the chemical composition. These calculations would inevitably produce the respective energetically most favorable ensembles. In the studied ceramic $\text{Si}_3\text{B}_3\text{N}_7$ this would imply an alternating occupation of the cation positions by silicon and boron. The need for an incorporation of the genesis of the amorphous network in the theoretical models begins to emerge.

Experimental Section

All solid-state NMR experiments were performed on a Bruker DSX400 NMR spectrometer operating at 9.4 T equipped with a 4 mm triple-resonance probe. The resonance frequencies were 128.35 MHz for ^{11}B and 79.46 MHz for ^{29}Si . All MAS measurements were performed at room temperature at a rotational frequency of 10 kHz.

^{29}Si -isotopically pure $\text{Si}_3\text{B}_3\text{N}_7$ was prepared from isotopically labeled [^{29}Si]trichlorosilylaminodichloroborane (TADB). $^{29}\text{SiCl}_4$, which was obtained by heating a mixture of elemental ^{29}Si and $\text{Pb}^{14}\text{Cl}_2$ at 600 °C, was allowed to react with hexamethyldisilazane (HMDS) in a ratio of 1:1 to give 1,1,1-trichloro-3,3,3-trimethyldisilazane (TTDS). Reaction of TTDS with BCl_3 finally led to the target molecule TADB. Condensation of TADB was performed using ammonia. Ammonium chloride, which formed as a by-product in the polymerization, was removed by sublimation at 500 °C.

Received: December 27, 1999 [Z14467]

- [1] a) M. Jansen, *Solid State Ionics* **1997**, 101–103, 1; b) H.-P. Baldus, M. Jansen, *Angew. Chem.* **1997**, 109, 338–354; *Angew. Chem. Int. Ed. Engl.* **1997**, 36, 328–343.
- [2] P. Baldus, M. Jansen, D. Sporn, *Science* **1999**, 285, 699–703.
- [3] G. Jeschke, M. Kroschel, M. Jansen, *J. Non-Cryst. Solids* **1999**, 260, 216–227.
- [4] D. Heinemann, W. Assenmacher, W. Mader, M. Kroschel, M. Jansen, *J. Mater. Res.* **1999**, 14, 3746–3753.
- [5] a) K. R. Carduner, C. S. Blackwell, W. B. Hammond, F. Reidinger, G. R. Hatfield, *J. Am. Chem. Soc.* **1990**, 112, 4676; b) A. H. Silver, P. J. Bray, *J. Chem. Phys.* **1960**, 32, 288; c) P. S. Marchetti, D. Kwon, W. R. Schmidt, L. V. Interrante, G. E. Maciel, *Chem. Mater.* **1991**, 3, 482.
- [6] a) T. Gullion, J. Schaefer, *J. Magn. Reson.* **1989**, 81, 196–200; b) T. Gullion, *Magn. Reson. Rev.* **1997**, 17, 83–131.
- [7] a) L. van Wüllen, B. Gee, L. Züchner, M. Bertmer, H. Eckert, *Ber. Bunsen Ges. Phys. Chem.* **1996**, 100, 1539–1549; b) L. van Wüllen, L. Züchner, W. Müller-Warmuth, H. Eckert, *Solid State NMR* **1996**, 6, 203–212.
- [8] a) A. Naito, K. Nishimura, S. Tuzi, H. Saito, *Chem. Phys. Lett.* **1994**, 229, 506–511; b) J. M. Goetz, J. Schaefer, *J. Magn. Reson.* **1997**, 117, 147–154; c) J. C. C. Chan, M. Bertmer, H. Eckert, *J. Am. Chem. Soc.* **1999**, 121, 5238–5248.
- [9] R. M. Hagenmayer, U. Müller, C. J. Benmore, J. Neufeind, M. Jansen, *J. Mater. Chem.* **1999**, 9, 2865–2870.

Tecto-RNA: One-Dimensional Self-Assembly through Tertiary Interactions**

Luc Jaeger* and Neocles B. Leontis*

The pioneering work of Seeman has demonstrated the use of DNA to construct nanoscale structures.^[1–3] Recent work extends these ideas to the assembly of noncovalent complexes, avoiding covalent ligation steps.^[4–6] While more chemically labile than DNA, RNA appears to offer a wider range of tertiary motifs^[7] that can be used as modular units for supramolecular engineering.^[8, 9] “RNA-tectonics” refers to the modular character of natural RNA molecules, which can be decomposed and reassembled to create new nanoscale molecular objects. The properties of RNA that facilitate its use in exploring new paradigms in nanoscale chemical self-assembly include (1) ease of sequence-specific synthesis (using either template-driven enzymatic methods or solid-phase chemical methods); (2) amenability of secondary and, increasingly, tertiary structure to rational design;^[9] (3) hierarchical folding of individual molecules;^[10] and (4) ability to participate in highly specific tertiary interactions.

Here we report the modular design and synthesis of RNA molecules capable of selective dimerization and one-dimensional self-assembly (Scheme 1). In contrast to associations involving Watson–Crick pairings, association occurs by specific tertiary interactions involving hairpin tetraloops and their receptors, as confirmed by lead(II)-cleavage protection experiments and by motif-swapping experiments.

We chose the specific “11-nucleotide motif” receptor for 5'-GAAA-3' tetraloops,^[11, 12] as the primary unit to mediate specific, high-affinity intermolecular RNA interactions. We first designed the self-dimerizing molecule **1**, RL-GAAA (Figure 1). All RNA molecules were synthesized by in vitro transcription of PCR-generated DNA templates (see Supporting Information) using T7 RNA polymerase. The self-association of **1**, as monitored by nondenaturing polyacrylamide gel electrophoresis, occurred with submicromolar dissociation constants and definitely required magnesium ions. At 15 mM $\text{Mg}(\text{OAc})_2$, **1** dimerized with $K_d = 4.3 \pm 0.4$ nM (Figure 2). The binding affinity of **1** was measured as a

[*] Dr. L. Jaeger
Institut de Biologie Moléculaire et Cellulaire
UPR 9002 du CNRS, 15 rue René Descartes
67084 Strasbourg Cedex (France)
Fax: (+33)03-88-60-22-18
E-mail: L.Jaeger@ibmc.u-strasbg.fr
Prof. N. B. Leontis
Chemistry Department
Center for Biomolecular Sciences
Bowling Green State University
Bowling Green, OH 43403 (USA)
Fax: (+1)419-372-9809
E-mail: leontis@bgnet.bgsu.edu

[**] This work was carried out in Strasbourg with the support of grants to N.B.L. from the NIH (1R15GM55898) and the NIH Fogarty Institute (1-F06-TW02251-01) and the support of the CNRS to L.J. The authors wish to thank Eric Westhof for his support and encouragement of this work.



Supporting information for this article is available on the WWW under <http://www.wiley-vch.de/home/angewandte/> or from the author.